



Reevaluation of
stratospheric ozone
trends from SAGE II
data

R. P. Damadeo et al.

Reevaluation of stratospheric ozone trends from SAGE II data using a simultaneous temporal and spatial analysis

R. P. Damadeo, J. M. Zawodny, and L. W. Thomason

NASA Langley Research Center, Hampton, VA, USA

Received: 2 June 2014 – Accepted: 22 June 2014 – Published: 2 July 2014

Correspondence to: R. P. Damadeo (robert.damadeo@nasa.gov)

Published by Copernicus Publications on behalf of the European Geosciences Union.

Title Page

Abstract

Introduction

Conclusions

References

Tables

Figures



Back

Close

Full Screen / Esc

Printer-friendly Version

Interactive Discussion



Abstract

This paper details a new method of regression for sparsely sampled data sets for use with time-series analysis, in particular the Stratospheric Aerosol and Gas Experiment (SAGE) II ozone data set. Non-uniform spatial, temporal, and diurnal sampling present in the data set result in biased values for the long-term trend if not accounted for. This new method is performed close to the native resolution of measurements and is a simultaneous temporal and spatial analysis that accounts for any potential diurnal variation. Results show declines in ozone similar to other studies but very different trends in the recovery period. The regression model allows for a variable turnaround time and reveals a hemispheric asymmetry in the middle to upper stratosphere. Similar methodology is also applied to SAGE II aerosol optical depth data to create a new volcanic proxy that covers the SAGE II mission period. Ultimately this technique may be extensible towards the inclusion of multiple data sets without the need for homogenization.

1 Introduction

The Stratospheric Aerosol and Gas Experiment (SAGE) II flew onboard the Earth Radiation Budget Satellite (ERBS) for over 20 years from its launch in October 1984 until its retirement in August 2005. It employed the solar occultation technique to measure multi-wavelength slant-path atmospheric transmission profiles at seven channels during each sunrise and sunset encountered by the spacecraft. During its operation, SAGE II produced high precision vertical profiles of atmospheric ozone ($\sim 1\%$) with excellent vertical resolution (~ 1 km) (Damadeo et al., 2013). The combination of accurate measurements and a long data record has seen SAGE II data consistently used for long-term ozone trend analysis (e.g., WMO, 2011; SPARC, 2013). Traditionally this is performed via multiple linear regression of monthly zonal mean ozone data to a set of predictor variables. However, given the sparse sampling of SAGE II measurements (~ 30 observations per day), biases can be introduced if the data are not carefully

Reevaluation of stratospheric ozone trends from SAGE II data

R. P. Damadeo et al.

Title Page

Abstract

Introduction

Conclusions

References

Tables

Figures



Back

Close

Full Screen / Esc

Printer-friendly Version

Interactive Discussion



treated. Herein we present a new way to perform time-series analysis on a sparsely sampled data set, in particular SAGE II, and compare the results and influence on trends with monthly zonal mean methods. The method outlined in this paper is similar to that of Bodeker et al. (2013) in that it utilizes a simultaneous temporal and spatial regression (though the terms used and how the regression is applied are different), but differs fundamentally in that it regresses to mean values of daily measurement swaths.

2 Predictor variables

The choices of predictor variables are important and thus are chosen based off of atmospheric variability that ozone has historically shown to be responsive to, namely: seasonal cycle, quasi-biennial oscillation (QBO), El Niño southern oscillation (ENSO), solar variability, volcanic eruption, and long-term trend terms. Ideally, each predictor variable is orthogonal to each other predictor variable. Since this is almost never the case, predictor variables are pretreated to create normalized orthogonal functions from multiple component data sets using empirical orthogonal function (EOF) analysis (also known as principal component analysis). When the use of EOF analysis becomes impossible due to having only one component data set, an orthogonal function is created by shifting the original function in time until the dot product between the shifted function and original function is zero over the overlap period, henceforth referred to as the temporal shift method. The use of orthogonal functions for predictors is better than the use of a single term because it allows the regression model to account for both magnitude and phase changes in the response.

With these tools in mind, a full set of predictor variables are created from component data sets in order to reduce the amount of multicollinearity. The seasonal cycle is simply a Fourier series with periods of 12 (annual), 6, 4, and 3 months (semiannual). To create a set of QBO predictor variables, EOF analysis is performed on compiled monthly mean equatorial wind data (<http://www.geo.fu-berlin.de/en/met/ag/strat/produkte/qbo/>) at seven pressure levels (70, 50, 40, 30, 20, 15, and 10 hPa), resulting in seven or

Reevaluation of stratospheric ozone trends from SAGE II data

R. P. Damadeo et al.

Title Page

Abstract

Introduction

Conclusions

References

Tables

Figures



Back

Close

Full Screen / Esc

Printer-friendly Version

Interactive Discussion



Reevaluation of stratospheric ozone trends from SAGE II data

R. P. Damadeo et al.

Title Page

Abstract

Introduction

Conclusions

References

Tables

Figures



Back

Close

Full Screen / Esc

Printer-friendly Version

Interactive Discussion



ozone measurements, so in theory these data could be used as a predictor variable. However these data have noise that is autocorrelated, making it a poor choice for use as a predictor variable. In addition, the effects of aerosol on ozone are not purely local (i.e. chemical reactions with local aerosol) but also dependent upon radiative effects from aerosol layers above and below the altitude layer in question. In the end, we chose to create our own volcanic predictor variable based off of stratospheric aerosol optical depth in the 1020 nm channel. This procedure is described in Appendix A.

In addition to predictor variables that act as proxies for geophysical variability, a number of cross-terms can also be considered. In the end, only one is included. The data used for the QBO proxy comes from equatorial data up to an altitude of ~ 32 km. However, it has been shown that the frequencies at which the QBO oscillates are different at higher latitudes than at the equator (Tung and Yang, 1994) and at higher altitudes (Remsberg and Lingenfelter, 2010). While the use of a proxy is better than simply using oscillating functions of different frequencies (since the QBO changes frequencies over time) and the use of orthogonal functions allows for the change in amplitude and phase of the response, it cannot account for the change in frequencies. In other words, regressing a QBO proxy from the equator at higher latitudes will not capture all of the variation, nor will regressing a QBO proxy from lower altitudes at higher altitudes even at the equator. It has been shown however (Tung and Yang, 1994), that the annual cycle modulates the QBO at higher latitudes, and thus the inclusion of this cross-term would better fit the response of ozone to the QBO at higher latitudes. Ideally a multi-dimensional QBO proxy would be used that captures global variability, but to the authors' knowledge, no such proxy exists.

3 Pretreatment of data

3.1 SAGE II observations

SAGE II was launched into a 57° inclined orbit and took two measurements per orbit. Each measurement was either a sunrise or sunset as seen by the spacecraft (spacecraft event type) and also either a sunrise or sunset as would be seen by an observer on the ground (local event type). Most of the time the spacecraft and local event types are the same, except at high latitudes. Given the nature of the orbit and observation technique, the instrument took measurements in two ground-track swaths across the surface of the Earth in a given day: one made of spacecraft sunrises and one made of spacecraft sunsets. Each swath spans about 3° to 10° in latitude for high to low latitudes respectively, and ~ 360° in longitude.

3.2 Data filtering

For the purpose of this paper, the same basic methodology is applied to the same source data with the difference being how that data is pretreated. The process begins by extracting SAGE II version 7.0 ozone (O₃) number density profiles for all non-dropped events and for all altitudes above the reported tropopause. A modification of the Wang et al. (2002) filtering criteria are applied, which includes the following: exclusion of any profile where the O₃ uncertainty exceeds 10% between 30 and 50 km, exclusion of all data below where the O₃ uncertainty exceeds 200% below 30 km, and exclusion of any data where the O₃ uncertainty exceeds 100% above 30 km. These filtering criteria also include aerosol filters to remove data within and below clouds (typically within the troposphere) and also to remove periods of heavy aerosol interference from the Pinatubo eruption. However, since this regression includes a volcanic term, data within the eruptive periods are not filtered out via aerosol criteria.

Reevaluation of stratospheric ozone trends from SAGE II data

R. P. Damadeo et al.

Title Page

Abstract

Introduction

Conclusions

References

Tables

Figures



Back

Close

Full Screen / Esc

Printer-friendly Version

Interactive Discussion



3.3 Data binning

The binning of data is one of the primary differences between the two methods. The first method, henceforth referred to as MZM (monthly zonal mean), is simply to take all data within a latitude bin (in this case 10° wide) and within a particular month and compute the mean value at each altitude. The time associated with this mean value is the center of the month and the latitude is the center of the bin. Different event types are not separated for these monthly zonal means. The second method, henceforth referred to as STS (simultaneous temporal and spatial), utilizes the data on a daily basis for each altitude. For each day, the events are separated into four subsets governed by the combination of local and spacecraft sunrises and sunsets (most of the time each day only contains two subsets of events). The mean of each subset is taken and the time associated with each mean is at the center of the day and the latitude is the mean of the latitudes of each event in the subset. The time of day is actually irrelevant here, since no diurnal model is used and each daily mean is already separated by event type, which will be treated differently as shown later.

3.4 Data averaging

We can consider, for each subset of events that we are taking a mean, that we have a collection of N data points (Y). The daily mean and standard deviation of the mean are simply the following:

$$\bar{Y} = \frac{1}{N} \sum_{i=1}^N Y_i \quad (1)$$

$$\sigma_{\bar{Y}} = \sqrt{\frac{1}{N(N-1)} \sum_{i=1}^N (Y_i - \bar{Y})^2} \quad (2)$$

Each data point also has some uncertainty value (δ) such that:

$$\delta_{\bar{Y}} = \frac{1}{N} \sqrt{\sum_{i=1}^N \delta_i^2} \quad (3)$$

So that, for each subset, the mean value η is simply \bar{Y} and the uncertainty in η is:

$$\delta_{\eta} = \sqrt{\sigma_{\bar{Y}}^2 + \delta_{\bar{Y}}^2} \quad (4)$$

In this way, the uncertainty in the daily or monthly mean is representative both of the uncertainty in the measurements as well as the overall variance. This is important, particularly at higher latitudes where it is possible one or two measurements of a subset dip into the vortex and produce abnormally low values that are not representative of the entire zonal band.

4 Regression methodology

After filtering and binning the data for both the MZM and STS methods, the following functional form is regressed to the data:

$$\eta(\theta, t) = \Theta(\theta)T(t) \quad (5)$$

where η is the concentration of O_3 , $\Theta(\theta)$ is the functional form of the latitude dependence, and $T(t)$ is the functional form of the temporal dependence. The measure of time for the purposes of regression is year fraction (e.g. 1994.65). This regression is done separately for each altitude. For the MZM method, $\Theta(\theta)$ is identically 1, since the data is regressed separately within each latitude band. For the STS method, $\Theta(\theta)$ is a series of seven Legendre polynomials in spherical harmonics (no longitudinal dependence). The temporal dependence is simply the sum of all of the predictor variables

plus a constant. However, the STS method also includes a conditional term based off of the local event type. This accounts for any differences in the mean values between sunrise and sunset events based off of diurnal variation in the data be it geophysical or algorithmic in origin.

5 The regression technique outlined in Appendix B is applied. Due to the nature of the data, very careful consideration is given when calculating the autocorrelation coefficient ϕ for the STS regression method. Only daily means with the same satellite event type can be correlated, and even then the temporal and spatial separation must be considered. We make the assumption that the level of autocorrelation does not change
10 significantly over sufficiently small separations, because the amount of autocorrelation is related to geophysical variability that is not well modeled, which is nearly constant over sufficiently small time and spatial scales. Thus, any consecutive data points that are within 5 days and 20° in latitude are included in the calculation of ϕ . No dependence upon the temporal or spatial separation was found within these limiting criteria
15 and so a simple lag-1 autocorrelation was still considered. In this way, a set of pairs of points was created for each event type, which were then all fed into the calculation of ϕ to determine a single value for use in the correction. The autocorrelation correction is then iterated until ϕ converges to within 0.05.

To account for the iterative correction of the heteroscedasticity, it was assumed that
20 values of k in Eq. (B13) had a simultaneous spatial and seasonal dependence (or purely seasonal for the MZM method). Regression was thus performed to a combination of the seasonal and spatial predictor variables. The fit to this data was used as the values of k and this process is iterated until k converges to values sufficiently near 1.

Residual filtering is performed using the deweighted, uncorrelated residuals (ϵ in
25 Eq. (B7), which have zero mean and unit variance) to remove outliers in the data. In order to create a filtering criteria, the median absolute deviation (MAD) is computed (Muller, 2000). Values of ϵ that deviate from the median by six MADs are omitted in future processing. Because residual filtering is performed on the deweighted, uncorrelated residuals, only data that both disagree with the model and are highly uncorrelated

Reevaluation of stratospheric ozone trends from SAGE II data

R. P. Damadeo et al.

Title Page

Abstract

Introduction

Conclusions

References

Tables

Figures



Back

Close

Full Screen / Esc

Printer-friendly Version

Interactive Discussion



with any other data are omitted. This process is iterated and the number of additional data points omitted decreases after each iteration. Since the filtering is performed with the use of MADs instead of standard deviations, an iteration can converge to exclude no additional data points, though in practice only a few iterations are required.

When performing regressions to data of this type, a common problem can be the excess of predictor terms. To overcome this, one can use a priori knowledge of what terms are and are not significant, or one can use all terms and manually determine which terms are statistically insignificant and omit those terms. This can, however, prove to be a tedious process, particularly when performing the same regression repeatedly for multiple latitudes and altitudes and with potentially several hundred terms. We instead choose to automate this process. A predictor term could be considered statistically significant if it is statistically different from zero at the two-sigma ($\sim 95\%$) level. In other words, if the ratio of the one-sigma uncertainty in a coefficient (σ_{β_j}) to the coefficient itself (β_j) is less than 0.5, it can be considered significant. After the residual filtering process is completed, an analysis of this ratio is done. During the first iteration, all coefficients with a ratio greater than 8 are omitted from future processing and the entire process is repeated (from the beginning). This threshold is iteratively lowered until only those coefficients that are statistically significant at the two-sigma level remain. In this way, all final coefficients are statistically significant at the two-sigma level. This does not, however, mean that all resulting terms are non-negligible. Though excluding predictor terms that are negligible (i.e. their contribution to the overall variance is minimal) is, in practice, unnecessary. Additionally, while each coefficient is statistically significant at the two-sigma level, groups of terms (e.g. piecewise linear slopes or EESC) can collectively become statistically insignificant depending upon their interactions.

Reevaluation of stratospheric ozone trends from SAGE II data

R. P. Damadeo et al.

Title Page

Abstract

Introduction

Conclusions

References

Tables

Figures



Back

Close

Full Screen / Esc

Printer-friendly Version

Interactive Discussion



Reevaluation of stratospheric ozone trends from SAGE II data

R. P. Damadeo et al.

Title Page

Abstract

Introduction

Conclusions

References

Tables

Figures



Back

Close

Full Screen / Esc

Printer-friendly Version

Interactive Discussion



range in latitude at the equator than at higher latitudes. The difference between the total and uncorrelated residuals are the correlated residuals. These correlated residuals are a measure of the discrepancy between the model and the data. Namely, they are a result of the geophysical variability that is well sampled but not well modeled as well as any instrumental variability (e.g. biased meteorological or ephemeris input data). This approach is useful, because applying the same model to different data sets could be used to independently assess the quality of the measurements via the uncorrelated residuals, as well as to ascertain deficiencies in the model or the data itself via analysis of the total residuals. A preliminary version of this technique was applied in Damadeo et al. (2013) to both the previous (v6.2) and current (v7.0) versions of the SAGE II data set to demonstrate and assess improvements made to the new version.

5.2 Predictor coefficient analysis

One of the problems with multiple linear regression is the issue of multicollinearity, or the possibility that two or more predictors are highly correlated. Multicollinearity, or even the presence of any correlation between predictors, does not affect the regression results as a whole (short of the possibility of poor inversion for numerical algorithms), but it does affect the interpretation of individual predictors. For example, if aerosol data was used (instead of just a volcanic proxy) that had an annual cycle in addition to the fitting of an annual cycle term, the annual cycle term would be biased because some of the annual variation in ozone would be attributable to the aerosol term. Fortunately, this effect is captured in the uncertainties in the predictor coefficients, but it still illustrates a problem when attempting to interpret single predictor coefficients. One could analyze the covariance matrix that results from the regression to determine the level of correlation between predictors, but nonetheless, care should be taken when interpreting results.

Due to these possible shortcomings, the analysis of any single predictor requires the analysis of all of the predictors in order to ensure they are reasonable. The annual cycle is fairly trivial with the exception of some overfitting in regions of missing data

(Fig. 1) and ENSO lacks any substantial contribution above 20 km (not shown). Since long-term trends are discussed later, this section will take a brief look at the remaining influential terms: QBO, solar cycle, and volcanic. It has been shown that SAGE II data quality is best between 20 and 50 km (Damadeo et al., 2013) and there are fewer gaps in sampling below 60° in latitude. As such, the following analysis will focus on this region.

5.2.1 QBO

After the annual cycle, the QBO is the largest source of variation in ozone. Figure 4 shows the amplitude of the response of ozone to the QBO as a function of latitude and altitude as a percentage of the local mean value (i.e. the mean value is a function of latitude and altitude). The amplitude is computed as the root mean square amplitude multiplied by $\sqrt{2}$, and is analogous to half of the peak-to-peak amplitude for a sine wave. As can be seen, the influence of the QBO is largest in the tropics in the lower and middle stratosphere as well as in the middle stratosphere at mid-latitudes. Figure 5 shows examples of the QBO term at the equator as a function of time and altitude and at 23 km as a function of time and latitude. The altitude dependent and latitude dependent phase lags are easily noticeable in the two figures. However, it should be noted that some deficiencies still remain due to the fact that the QBO proxy term originated from data at the equator. The frequencies at altitudes above the proxy do not change and the frequencies at mid-latitudes are slightly different only because of the inclusion of a cross-term with the annual cycle. It should also be noted that the amplitude of the QBO is larger near Pinatubo, which may be a physical response of the QBO itself to the Pinatubo eruption (Thomas et al., 2009) or it may simply be a byproduct of correlation with that term. Additionally, the fact that the regression is both temporal and spatial means that the inability to accurately model the QBO at higher latitudes will detract from the ability to accurately model the QBO at lower latitudes.

Reevaluation of stratospheric ozone trends from SAGE II data

R. P. Damadeo et al.

Title Page

Abstract

Introduction

Conclusions

References

Tables

Figures



Back

Close

Full Screen / Esc

Printer-friendly Version

Interactive Discussion



5.2.2 Solar

To include a response of ozone to the solar cycle, the regression model can include either one or two solar predictor variables. The biggest differences between one or two terms are seen in the tropics between 25 and 35 km. The amplitudes of the oscillation are similar, as shown in Fig. 6, with the exception of a very weak oscillation in this region if only a single term is used. This is because, when two terms are used, the solar term, if allowed to change phase, exhibits strong correlations with the volcanic term in this region as shown in Fig. 7. Here, the solar cycle is shifted later in phase by about two years to coincide with the peak of volcanic increase surrounding the Pinatubo eruption, which is similar to results shown in Remsberg (2014).

The inclusion of a volcanic term reduces the overall residuals regardless of whether one or two solar terms are included (not shown), but there is a negligible difference in residuals between the use of one or two solar terms if a volcanic term is also used. It is unclear if the response of ozone to the solar cycle really does lag by about two years in the mid-stratosphere in the tropics or if the algorithm is simply trying to attribute some of the response of ozone to aerosol to the solar cycle instead.

5.2.3 Volcanic

The results of the volcanic term need to be interpreted very carefully. On one hand it is clear from the data that ozone responds to changes in aerosol, particularly near Pinatubo. On the other hand, the SAGE II inversion algorithm can produce biases in ozone in the presence of high aerosol loading (Damadeo et al., 2013) and so some of the response to aerosol, particularly at lower altitudes in the tropics, can have algorithmic rather than physical origins. However, omitting data based off of aerosol extinction (e.g. Wang et al., 2002) and assuming that the influence of aerosol has been removed would be incorrect.

A look at the response of ozone near the Pinatubo eruption reveals both physical and algorithmic responses as well as regressive responses. Figure 8 shows the peak

Reevaluation of stratospheric ozone trends from SAGE II data

R. P. Damadeo et al.

Title Page

Abstract

Introduction

Conclusions

References

Tables

Figures



Back

Close

Full Screen / Esc

Printer-friendly Version

Interactive Discussion



differences between sunrise and sunset events accounts for this effect and results in smaller recovery trends in the STS method.

It is clear that the differences caused by the SAGE II non-uniform sampling are important, and that the STS method is preferable to the MZM method regardless of which long-term trend term is used. However, there are still some differences in trends between the two terms as shown in Figs. 12 and 13. To understand this, one needs to look at the time evolution of the long-term trend for the use of each term. Figure 14 illustrates the difference between the two terms at 50° N. The piecewise linear trend term forces any turnaround in ozone to occur at 1997, while the use of the two orthogonal EESC terms allows this turnaround point to move in time. As shown in Fig. 14 (top right), the turnaround time is earlier at lower altitudes. This is consistent with the fact that stratospheric ozone is inversely related to stratospheric chlorine, and the EESC proxies from Newman et al. (2007) show that the EESC peaks earlier for smaller mean ages of air. Figure 14 would suggest then, that the mean age of air in the Northern Hemisphere decreases with decreasing altitude, which is consistent with results shown in Waugh and Hall (2002).

The study outlined in Waugh and Hall (2002) is performed only for the Northern Hemisphere and the assumption is made that the hemispheres are symmetric. However, the time evolution of the long-term trend at high southern latitudes (Fig. 14, bottom right) shows no clear change in turnaround time with altitude, and in some cases never turns around (i.e. is always decreasing). It is, at present, unclear if this hemispheric asymmetry is geophysical or a result of correlation between the long-term trend and other terms (e.g. solar or volcanic).

8 Conclusions

A new method for performing time-series analysis of sparsely sampled data, in particular SAGE II, has been presented. The differences between the MZM method and the STS method have been discussed and the impacts on the long-term trends in ozone

Reevaluation of stratospheric ozone trends from SAGE II data

R. P. Damadeo et al.

Title Page

Abstract

Introduction

Conclusions

References

Tables

Figures



Back

Close

Full Screen / Esc

Printer-friendly Version

Interactive Discussion



Reevaluation of stratospheric ozone trends from SAGE II data

R. P. Damadeo et al.

Title Page

Abstract

Introduction

Conclusions

References

Tables

Figures



Back

Close

Full Screen / Esc

Printer-friendly Version

Interactive Discussion



detailed. It has been shown that the non-uniform sampling in SAGE II data will produce biased long-term trend values in ozone if not properly accounted for. The STS method shows declines in ozone that are similar to those from other studies in the upper stratosphere at middle to high latitudes but very different results for the recovery period, namely a noticeable decrease in the magnitude of recovery in the Southern Hemisphere. The use of two orthogonal EESC predictor variables instead of a piecewise linear trend allows for a variable turnaround time in ozone due to differing mean ages of air. Results show a hemispheric asymmetry in the middle to upper stratosphere, with an earlier turnaround time with lower altitude and latitude in the Northern Hemisphere but no coherent pattern in the Southern Hemisphere. It has also been shown that the STS method can be used to assess the quality of a data set's measurements independent of other data sets. In addition to ozone, the STS method was applied to SAGE II aerosol optical depth data to create a new volcanic proxy that covers the SAGE II mission period.

For future work, we would like to extend this technique to other ozone data sets as well as to include multiple data sets to better constrain the long-term trends in the recovery period. The benefit of this technique for the creation of a single time-series derived from multiple data sets is that it does not require the homogenization of the different data sets prior to regression. Instead, instrument-dependent conditional terms representing mean offsets, different diurnal variation, time-dependent drifts, or other terms could be included if necessary. Another consideration is to expand upon the creation of a volcanic proxy term to one that is altitude dependent, so that the response of ozone to both local (i.e. at the same altitude) and total aerosol can be assessed. Lastly, it could be beneficial to experiment with other coordinate systems in order to reduce uncertainties in regions of larger variance. For example, regression could be done on the data at its native resolution, using models for diurnal and longitudinal variation, as this would reduce some of the variance in the tropics where each daily mean spans $\sim 10^\circ$ in latitude as opposed to $\sim 3^\circ$ in latitude at high latitudes. Another coordinate transformation would be to perform this regression methodology on equivalent latitude

Reevaluation of stratospheric ozone trends from SAGE II data

R. P. Damadeo et al.

Title Page

Abstract

Introduction

Conclusions

References

Tables

Figures



Back

Close

Full Screen / Esc

Printer-friendly Version

Interactive Discussion



tion), followed by an increase in aerosol up to some peak value over time, followed lastly by a long decay back to background levels (unless another eruption occurs). It makes sense to create a piecewise function to model this rise and fall, but the choice of these functions is important. Previous attempts (e.g., SPARC, 2006, Chapter 5.4.2) use a simple polynomial from eruption to peak values followed by an exponential decay with some characteristic decay constant. However, a simple exponential decay model would assume that the data, when plotted in log-space, is linear, which it clearly is not (see Fig. 15).

While analyzing the logarithm of the aerosol data, we choose a piecewise pair of second order polynomials in order to fit the eruptive effects on aerosol. However, the two functions are restricted to maintain continuity of both the functions and their derivatives where they join, as well as to assume the eruptive term returns to zero (i.e. background) after some amount of time has elapsed. In this way, a pair of piecewise second order polynomials can be defined by the declaration of three parameters: time of injection (t_1 or time aerosol first arrives at a location after an eruption), peak time (t_P or time after injection at which aerosol values are at their peak), and return time (t_R or time after injection at which the eruptive term and its derivative returns to zero). The time at which these two functions join is also constrained by these three parameters.

The downside to this methodology is that the functional form of the eruptive term is not linearly dependent upon the parameter times (t_1 , t_P , and t_R). Additionally, the times themselves are functions of latitude and different for each eruption. Since we have no intrinsic knowledge of the value of these times, or their spatial dependence, a non-linear least squares fitting technique is applied to binned data. The process begins with data taken in a 10° wide bin in latitude centered at a particular latitude. Initial guesses are made for the three parameters for each of seven volcanic eruptions: El Chichon (1982), Nevado del Ruiz (1985), Kelut (1990), Pinatubo (1991), Cerro Hudson (1991), Ruang (2002), and Manam (2004). The MPFIT algorithm (Markwardt, 2009) is used, as it allows for restrictions on solvable parameters to be placed, which greatly aids in convergence. An insufficient amount of data is available to constrain t_1 or t_P

for El Chichon, so these parameters are tied to Pinatubo. Likewise, t_R for Manam was set constant at 5 years. Some examples of the non-linear regressions can be seen in Fig. 15.

This non-linear regression was performed for each latitude between 70° S and 70° N in increments of 1°. The parameters (t_I , t_P , and t_R) were then smoothed, and any iterations that did not converge properly were ignored. To create the eruptive terms for the STS regression, the parameters were interpolated (or held constant at last value for extrapolation) to all latitudes to create functional forms for each volcano for the entire record. These eruptive terms are then easily linearly regressed to, where the STS regression is allowed to determine spatial dependence but not temporal variation for each volcano as a function of latitude. The final product to be fed into the regression for ozone is a single volcanic term that represents the eruptive changes in aerosol at all times during the record for all latitudes (Fig. 16).

Ultimately the creation of a volcanic proxy is an empirical result. Theoretically, one could look at the parameters from the non-linear least squares regression individually, but most of the terms would have no real meaning. For example, there are a large number of volcanic eruptions around the time of the eruption of Nevado del Ruiz. While the parameters near the eruption make sense, the parameters at higher latitudes merely represent the algorithm's attempt to fit the overall increase in aerosol from a multitude of eruptions in that time period (e.g. $t_P \sim 2$ years and $t_R \sim 8$ years). The regression fits the overall data well, but each individual term is not necessarily representative of that eruption alone.

Appendix B

The principle of multiple linear regression is predicated upon the simple assumption that a dependent variable (Y) is linearly dependent upon a set of predictor variables

Reevaluation of stratospheric ozone trends from SAGE II data

R. P. Damadeo et al.

Title Page

Abstract

Introduction

Conclusions

References

Tables

Figures



Back

Close

Full Screen / Esc

Printer-friendly Version

Interactive Discussion



(X) that produce a simple equation of the following form:

$$Y = X\beta + R, \quad (B1)$$

where Y is a vector of N data points (index i), β is a vector of coefficients for M predictor variables that include a constant (index j), X is an N by M matrix of each predictor variable corresponding to each data point, and R is a vector of N residual differences between the data and the fit. It should be noted that generally $X_{i,j=0}$ is identically 1 for all i from 1 to N and $\beta_{j=0}$ is simply the overall constant of the fit. These coefficients can be solved for using a simple ordinary least squares (OLS) regression technique (Kutner et al., 2005). The uncertainties in the coefficients (σ_β) can also easily be solved for provided the following assumption holds:

$$\text{var}(Y) = \sigma_0^2 I, \quad (B2)$$

where $\text{var}(Y)$ denotes the variance-covariance matrix of Y , σ_0 is some constant, and I is the identity matrix. If this assumption holds, then the residuals have the property of being Gaussian with a constant conditional variance of σ_0^2 .

If the assumption of Eq. (B2) does not hold, then Eq. (B2) reverts to a general form:

$$\text{var}(Y) = \Sigma_0. \quad (B3)$$

This produces coefficients that are still unbiased, but the estimates of their uncertainties are biased small. To overcome this problem, we turn to generalized least squares (GLS), which applies a transformation matrix G to Eq. (B1) to obtain

$$Y^* = X^* \beta + R^*. \quad (B4)$$

If $G = \sigma_0^{-1} \Sigma_0^{-\frac{1}{2}}$ (where $\Sigma_0^{-\frac{1}{2}} \Sigma_0^{-\frac{1}{2}'} = \Sigma_0^{-1}$), then R^* has the property of being Gaussian with conditional variance σ_0^2 . The coefficients and their respective uncertainties can be

computed in the following way:

$$\beta = (\mathbf{X}'\Sigma_0^{-1}\mathbf{X})^{-1}\mathbf{X}'\Sigma_0^{-1}\mathbf{Y} = (\mathbf{X}^*\mathbf{X}^*)^{-1}\mathbf{X}^*\mathbf{Y}^* \quad (\text{B5})$$

$$\text{var}(\beta) = (\mathbf{X}'\Sigma_0^{-1}\mathbf{X})^{-1} = \sigma_0^2(\mathbf{X}^*\mathbf{X}^*)^{-1}. \quad (\text{B6})$$

5 It follows that σ_{β_j} is the square-root of the j^{th} diagonal element of Eq. (B6). It is worth noting that, when solved explicitly using Σ_0 , the values of the coefficients and their uncertainties are invariant to the value of σ_0 , but when a transformation of variables is used, the equations revert to the form of solutions from OLS regression.

10 In time series analysis it is often the case that the assumption of Eq. (B2) does not hold. The residuals are, in fact, both heteroscedastic (have a non-constant variance) and serially correlated (temporally autocorrelated). If we assume the residuals have the following properties:

$$R_i = \phi R_{i-1} + \sigma_i \epsilon_i, \quad (\text{B7})$$

15 where ϕ is the autocorrelation coefficient, R_i are the total residuals, ϕR_{i-1} are the correlated residuals, $\sigma_i \epsilon_i$ are the uncorrelated residuals, and ϵ is Gaussian with unit conditional variance, then Eq. (B2) reverts to Eq. (B3), where Σ_0 is an N by N symmetric matrix with components of the following form:

$$20 \Sigma_{0,i,j} = \frac{\sigma_i \sigma_j \phi^{|i-j|}}{1 - \phi^2}, \quad (\text{B8})$$

Reevaluation of stratospheric ozone trends from SAGE II data

R. P. Damadeo et al.

Title Page	
Abstract	Introduction
Conclusions	References
Tables	Figures
◀	▶
◀	▶
Back	Close
Full Screen / Esc	
Printer-friendly Version	
Interactive Discussion	



where, for this case, j goes from 1 to N . Computing \mathbf{G} leads to the following transformation of variables:

$$\begin{aligned}
 Y_i^* &= \frac{Y_i - \phi Y_{i-1}}{\sigma_i}, \\
 X_{i,j}^* &= \frac{X_{i,j} - \phi X_{i-1,j}}{\sigma_i}, \\
 R_i^* &= \frac{R_i - \phi R_{i-1}}{\sigma_i} = \epsilon_j.
 \end{aligned}
 \tag{B9}$$

This is just the Cochrane-Orcutt transformation (Cochrane and Orcutt, 1949), which ignores the first data point. The Prais-Winsten transformation (Prais and Winsten, 1954) can be used to include the first data point and an additional modification outlined in Savin and White (1978) can be used to account for data gaps. It should be noted that, when performing OLS regression to the transformed variables, it will be necessary to force regression about the origin if using a packaged algorithm that performs regression and always assumes a constant.

If the heteroscedasticity and autocorrelation are known precisely and everything about the regression is perfect, then theoretically $\sigma_0 = 1$. In reality this is never the case. A good estimate of σ_0 , however, can be obtained from the weighted mean-square error (also known as the reduced weighted chi-squared error statistic):

$$\sigma_0^2 = \frac{\mathbf{\epsilon}'\mathbf{\epsilon}}{N - M}
 \tag{B10}$$

It is important to compute σ_0 so as to not underestimate the uncertainties in the coefficients in Eq. (B6) when regressing to transformed variables.

In theory, one would want to know a priori what the values for ϕ and σ are. Instead, these parameters are solved for iteratively towards convergence. The value for the autocorrelation coefficient is solved for by first performing OLS regression and then

Reevaluation of stratospheric ozone trends from SAGE II data

R. P. Damadeo et al.

Title Page	
Abstract	Introduction
Conclusions	References
Tables	Figures
◀	▶
◀	▶
Back	Close
Full Screen / Esc	
Printer-friendly Version	
Interactive Discussion	



computing ϕ in the usual manner:

$$\phi = \frac{\sum_{i=1}^{N-1} (R_i - \bar{R})(R_{i-1} - \bar{R})}{\sum_{i=1}^N (R_i - \bar{R})^2}, \quad (\text{B11})$$

which is itself a simple modification of the Pearson product-moment correlation coefficient:

$$\phi(X, Y) = \frac{\sum_{i=1}^N (X_i - \bar{X})(Y_i - \bar{Y})}{\sqrt{\sum_{i=1}^N (X_i - \bar{X})^2} \sqrt{\sum_{i=1}^N (Y_i - \bar{Y})^2}} \quad (\text{B12})$$

As can be seen, X and Y have been substituted with adjacent values of the residuals as well as a slight modification of the limits of summation to account for the number of pairs vs. the number of total points.

The nature of the heteroscedasticity can be slightly more complicated. In practice, one only has an estimate for the heteroscedasticity (δ) such that:

$$\sigma_i = \delta_i k_i. \quad (\text{B13})$$

If the initial guess of the heteroscedasticity is correct, then k is identically 1. However, generally k is more complex, having a dependence on the predictor variables themselves. A practical way to solve for k is to first assume that $\sigma = \delta$ and solve for ϵ . If $k = 1$, then the mean value of ϵ^2 should also be 1. As such, one can regress a function $f = \log(\epsilon^2)$ to predictor variables and obtain a fit value (f_i) for each ϵ_i , then $k_i = \sqrt{e^{f_i}}$. In this way, σ can be iteratively updated until k converges towards 1. However, the choice of predictor variable dependence of k may or may not be straightforward.

Reevaluation of stratospheric ozone trends from SAGE II data

R. P. Damadeo et al.

Title Page	
Abstract	Introduction
Conclusions	References
Tables	Figures
◀	▶
◀	▶
Back	Close
Full Screen / Esc	
Printer-friendly Version	
Interactive Discussion	



Acknowledgements. The ongoing development, production, assessment, and analysis of SAGE data sets at NASA Langley Research Center is supported by NASA's Earth Science Directorate.

References

- 5 Bodeker, G. E., Hassler, B., Young, P. J., and Portmann, R. W.: A vertically resolved, global, gap-free ozone database for assessing or constraining global climate model simulations, *Earth Syst. Sci. Data*, 5, 31–43, doi:10.5194/essd-5-31-2013, 2013. 17683, 17695
- Bourassa, A. E., Degenstein, D. A., Randel, W. J., Zawodny, J. M., Kyrölä, E., McLinden, C. A., Sioris, C. E., and Roth, C. Z.: Trends in stratospheric ozone derived from merged SAGE
10 II and Odin-OSIRIS satellite observations, *Atmos. Chem. Phys. Discuss.*, 14, 7113–7140, doi:10.5194/acpd-14-7113-2014, 2014. 17697
- Cochrane, D. and Orcutt, G.: Application of least squares regression to relationships containing auto-correlated error terms, *J. Am. Stat. Assoc.*, 44, 32–61, doi:10.1080/01621459.1949.10483290, 1949. 17705
- 15 Damadeo, R. P., Zawodny, J. M., Thomason, L. W., and Iyer, N.: SAGE version 7.0 algorithm: application to SAGE II, *Atmos. Meas. Tech.*, 6, 3539–3561, doi:10.5194/amt-6-3539-2013, 2013. 17682, 17692, 17693, 17694, 17696
- Kutner, M. H., Nachtsheim, C. J., Neter, J., and Li, W.: *Applied Linear Statistical Models*, 5th edn., ISBN 0-07-238688-6, McGraw-Hill, Irwin, 2005. 17703
- 20 Kyrölä, E., Laine, M., Sofieva, V., Tamminen, J., Päivärinta, S.-M., Tukiainen, S., Zawodny, J., and Thomason, L.: Combined SAGE II–GOMOS ozone profile data set for 1984–2011 and trend analysis of the vertical distribution of ozone, *Atmos. Chem. Phys.*, 13, 10645–10658, doi:10.5194/acp-13-10645-2013, 2013. 17684, 17697
- Markwardt, C. B.: Non-linear least squares fitting in IDL with MPFIT, in: *Astronomical Data Analysis Software and Systems XVIII*, vol. 411, available at: <http://purl.com/net/mpfit> (last
25 access: 2014), 251–254, 2009. 17701
- Muller, J. W.: Possible advantages of a robust evaluation of comparisons, *J. Res. Natl. Inst. Stan.*, 105, 551–555, available at: <https://archive.org/details/jresv105n4p551>, 2000. 17689

Reevaluation of stratospheric ozone trends from SAGE II data

R. P. Damadeo et al.

Title Page

Abstract

Introduction

Conclusions

References

Tables

Figures



Back

Close

Full Screen / Esc

Printer-friendly Version

Interactive Discussion



Reevaluation of stratospheric ozone trends from SAGE II data

R. P. Damadeo et al.

Title Page

Abstract

Introduction

Conclusions

References

Tables

Figures



Back

Close

Full Screen / Esc

Printer-friendly Version

Interactive Discussion



Newman, P. A., Daniel, J. S., Waugh, D. W., and Nash, E. R.: A new formulation of equivalent effective stratospheric chlorine (EESC), *Atmos. Chem. Phys.*, 7, 4537–4552, doi:10.5194/acp-7-4537-2007, 2007. 17684, 17698

Prais, S. J. and Winsten, C. B.: Trend Estimators and Serial Correlation, available at: <http://cowles.econ.yale.edu/P/ccdp/st/s-0383.pdf>, Cowles Commission, Chicago, 1954. 17705

Randel, W. J. and Wu, F.: A stratospheric ozone profile data set for 1979–2005: variability, trends, and comparisons with column ozone data, *J. Geophys. Res.-Atmos.*, 112, D06313, doi:10.1029/2006JD007339, 2007. 17697

Remsberg, E. E.: Decadal-scale responses in middle and upper stratospheric ozone from SAGE II version 7 data, *Atmos. Chem. Phys.*, 14, 1039–1053, doi:10.5194/acp-14-1039-2014, 2014. 17694

Remsberg, E. and Lingenfelser, G.: Analysis of SAGE II ozone of the middle and upper stratosphere for its response to a decadal-scale forcing, *Atmos. Chem. Phys.*, 10, 11779–11790, doi:10.5194/acp-10-11779-2010, 2010. 17685

Savin, N. E. and White, K. J.: Testing for autocorrelation with missing observations, *Econometrica*, 46, 59–67, available at: <http://www.jstor.org/stable/1913645>, 1978. 17705

SPARC: Assessment of Stratospheric Aerosol Properties (ASAP), SPARC Report No. 4, WCRP-124, WMO/TD-No. 1295, available at: <http://www.atmosph.physics.utoronto.ca/SPARC/index.html>, 2006. 17700, 17701

SPARC: Lifetimes of Stratospheric Ozone-Depleting Substances, their Replacements, and Related Species, SPARC Report No. 6, WCRP-15/2013, available at: <http://www.atmosph.physics.utoronto.ca/SPARC/index.html>, 2013. 17682

Thomas, M. A., Giorgetta, M. A., Timmreck, C., Graf, H.-F., and Stenchikov, G.: Simulation of the climate impact of Mt. Pinatubo eruption using ECHAM5 – Part 2: Sensitivity to the phase of the QBO and ENSO, *Atmos. Chem. Phys.*, 9, 3001–3009, doi:10.5194/acp-9-3001-2009, 2009. 17693

Tung, K. K. and Yang, H.: Global QBO in circulation and ozone. Part I: Reexamination of observational evidence, *J. Atmos. Sci.*, 51, 2699–2707, 1994. 17685

Wang, H. J., Cunnold, D. M., Thomason, L. W., Zawodny, J. M., and Bodeker, G. E.: Assessment of SAGE version 6.1 ozone data quality, *J. Geophys. Res.-Atmos.*, 107, ACH 8-1–ACH 8-18, doi:10.1029/2002JD002418, 2002. 17686, 17694

Waugh, D. and Hall, T.: Age of stratospheric air: theory, observations, and models, *Rev. Geophys.*, 40, 1-1–1-26, doi:10.1029/2000RG000101, 2002. 17698

ACPD

14, 17681–17725, 2014

Reevaluation of stratospheric ozone trends from SAGE II data

R. P. Damadeo et al.

Title Page

Abstract

Introduction

Conclusions

References

Tables

Figures



Back

Close

Full Screen / Esc

Printer-friendly Version

Interactive Discussion



Reevaluation of stratospheric ozone trends from SAGE II data

R. P. Damadeo et al.

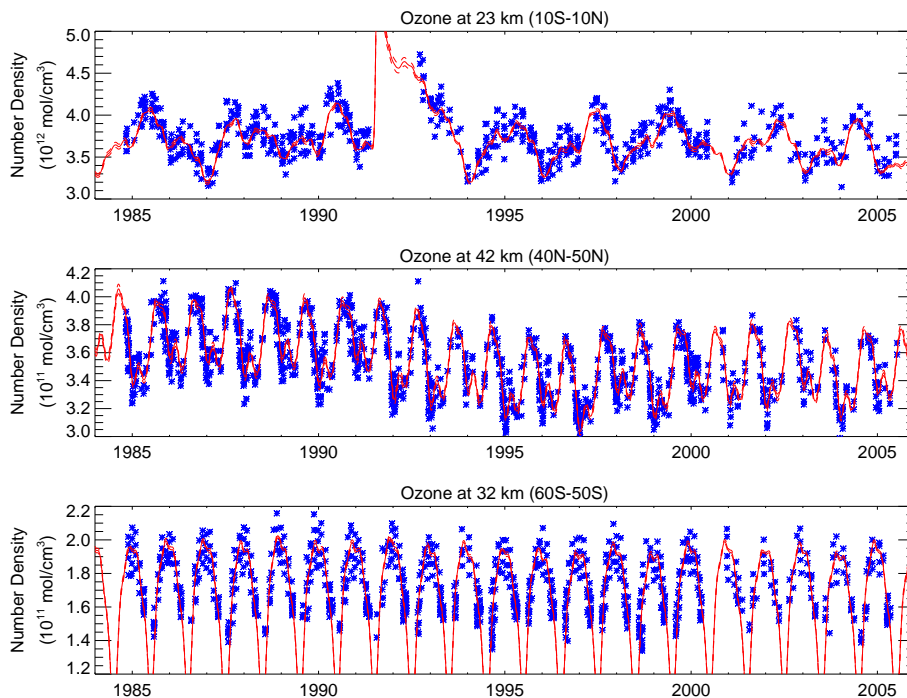


Figure 1. Some examples of the STS regression. Data within the stated latitude bin are shown in blue while a fit at the center of the bin is shown in red. The data shown have autocorrelation and diurnal variation removed for the purposes of plotting.

[Title Page](#)[Abstract](#)[Introduction](#)[Conclusions](#)[References](#)[Tables](#)[Figures](#)[Back](#)[Close](#)[Full Screen / Esc](#)[Printer-friendly Version](#)[Interactive Discussion](#)

Reevaluation of stratospheric ozone trends from SAGE II data

R. P. Damadeo et al.

Title Page

Abstract

Introduction

Conclusions

References

Tables

Figures

◀

▶

◀

▶

Back

Close

Full Screen / Esc

Printer-friendly Version

Interactive Discussion

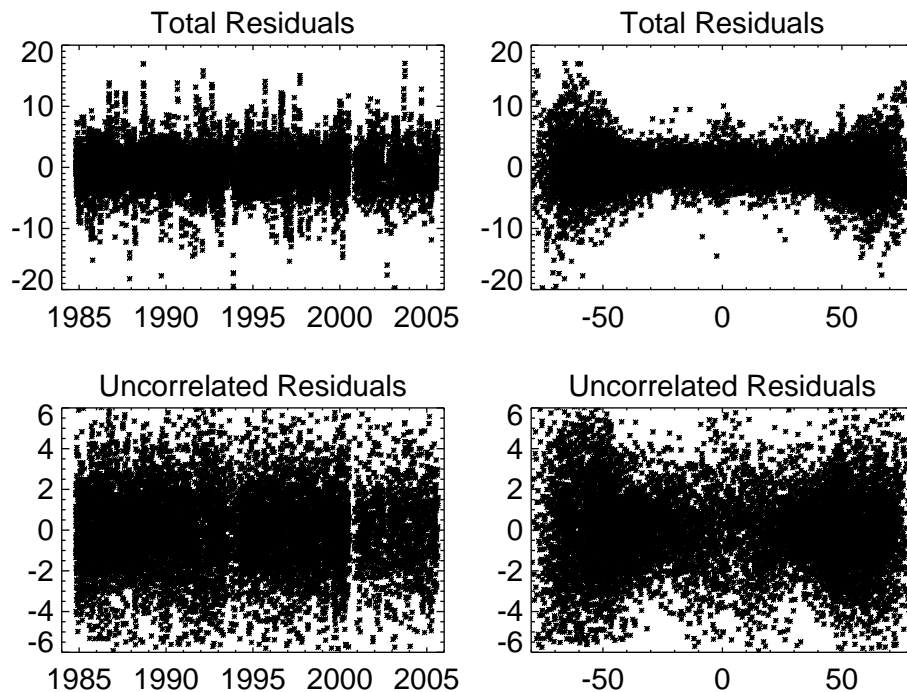


Figure 2. Total and uncorrelated residuals (as percents) as a function of both time and latitude at 25 km from the STS regression. Results are similar at other altitudes, though scales may change.

Reevaluation of stratospheric ozone trends from SAGE II data

R. P. Damadeo et al.

Title Page

Abstract

Introduction

Conclusions

References

Tables

Figures



Back

Close

Full Screen / Esc

Printer-friendly Version

Interactive Discussion

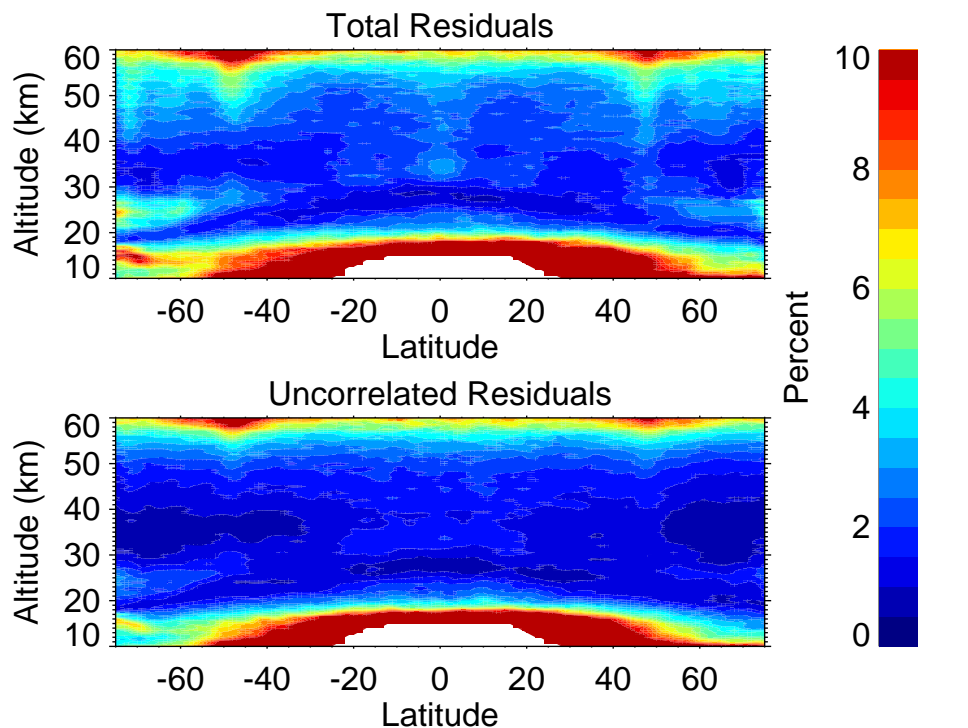


Figure 3. Spread of the total and uncorrelated residuals as a function of latitude and altitude from the STS regression. White regions show areas where insufficient data exists, generally due to being in the troposphere or early profile termination during retrievals.

Reevaluation of stratospheric ozone trends from SAGE II data

R. P. Damadeo et al.

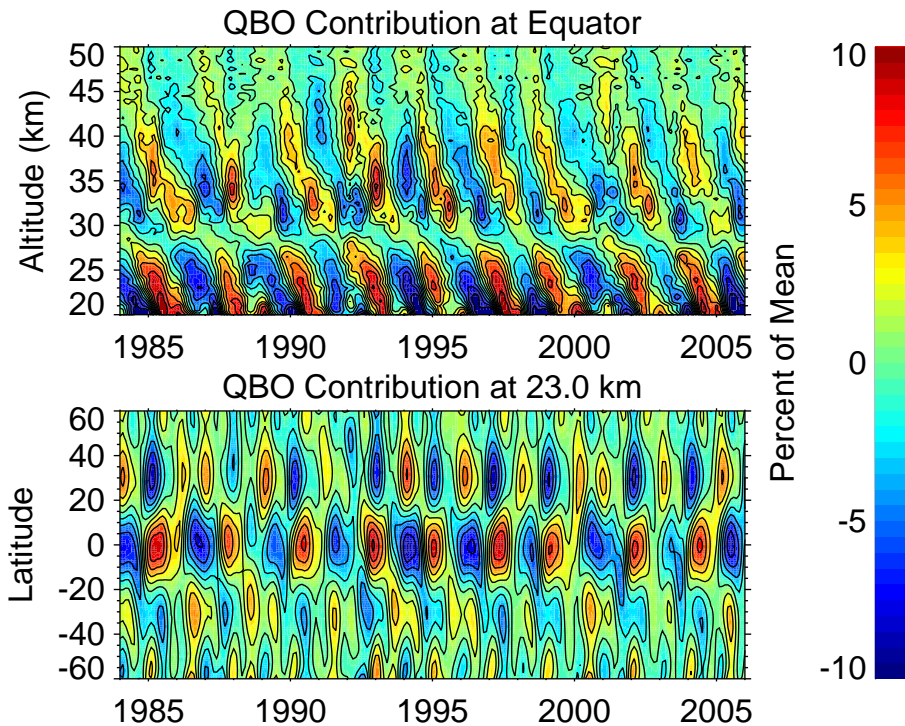


Figure 5. Examples of the QBO term. Contour lines are plotted at intervals of 2%.

Title Page

Abstract Introduction

Conclusions References

Tables Figures

◀ ▶

◀ ▶

Back Close

Full Screen / Esc

Printer-friendly Version

Interactive Discussion



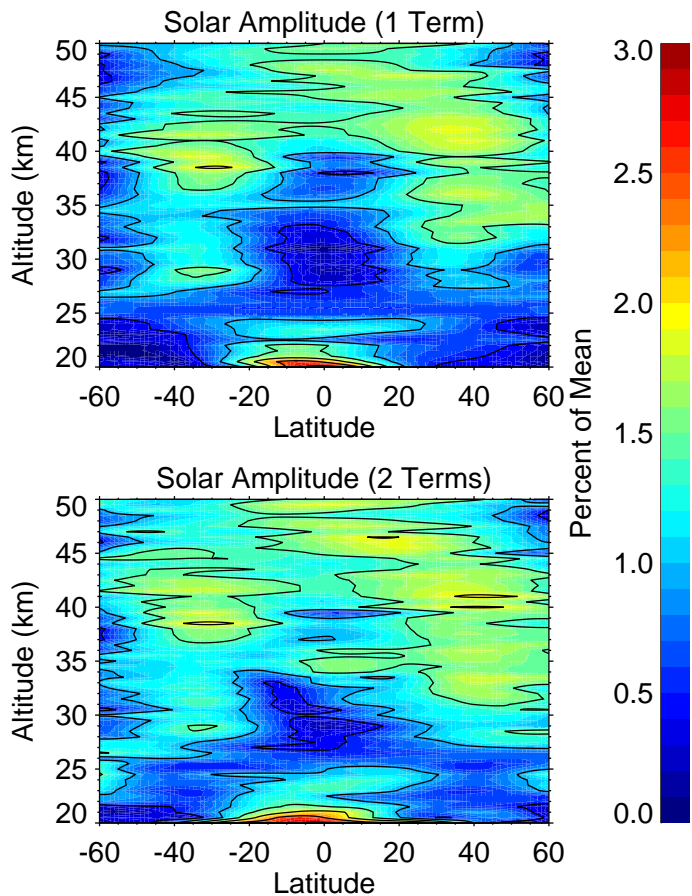


Figure 6. Amplitude of oscillation of the solar term as a percentage of the local mean for the use of one and two solar proxy terms while including a volcanic term. Contour lines are plotted at intervals of 0.5%.

Reevaluation of stratospheric ozone trends from SAGE II data

R. P. Damadeo et al.

Title Page

Abstract Introduction

Conclusions References

Tables Figures

◀ ▶

◀ ▶

Back Close

Full Screen / Esc

Printer-friendly Version

Interactive Discussion



Reevaluation of stratospheric ozone trends from SAGE II data

R. P. Damadeo et al.

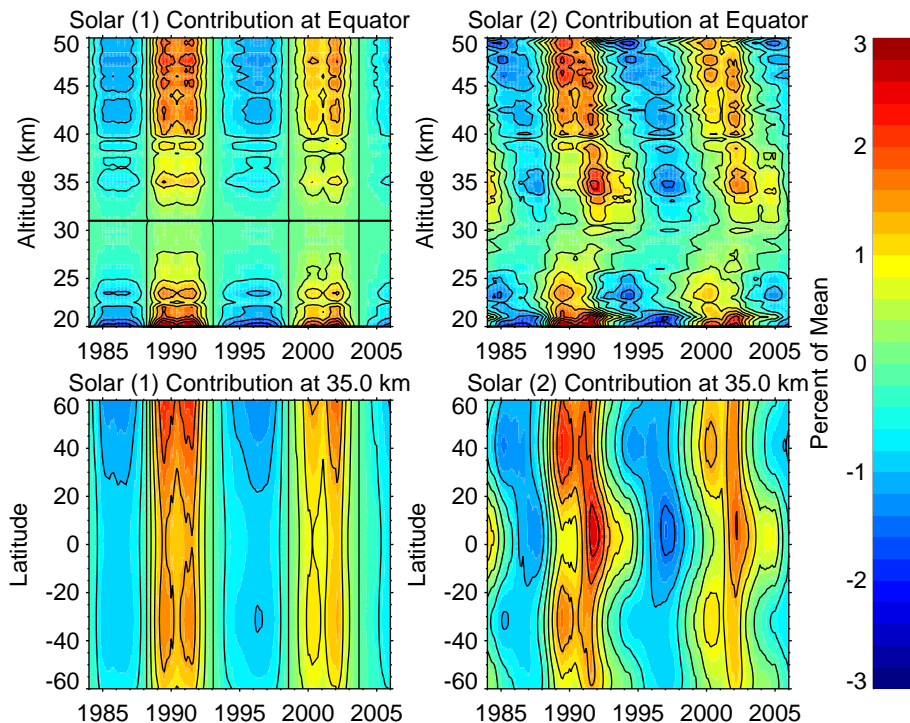


Figure 7. Examples of the solar term for the use of one and two solar proxy terms while including a volcanic term. Contour lines are plotted at intervals of 0.5 %.

[Title Page](#)[Abstract](#)[Introduction](#)[Conclusions](#)[References](#)[Tables](#)[Figures](#)[◀](#)[▶](#)[◀](#)[▶](#)[Back](#)[Close](#)[Full Screen / Esc](#)[Printer-friendly Version](#)[Interactive Discussion](#)

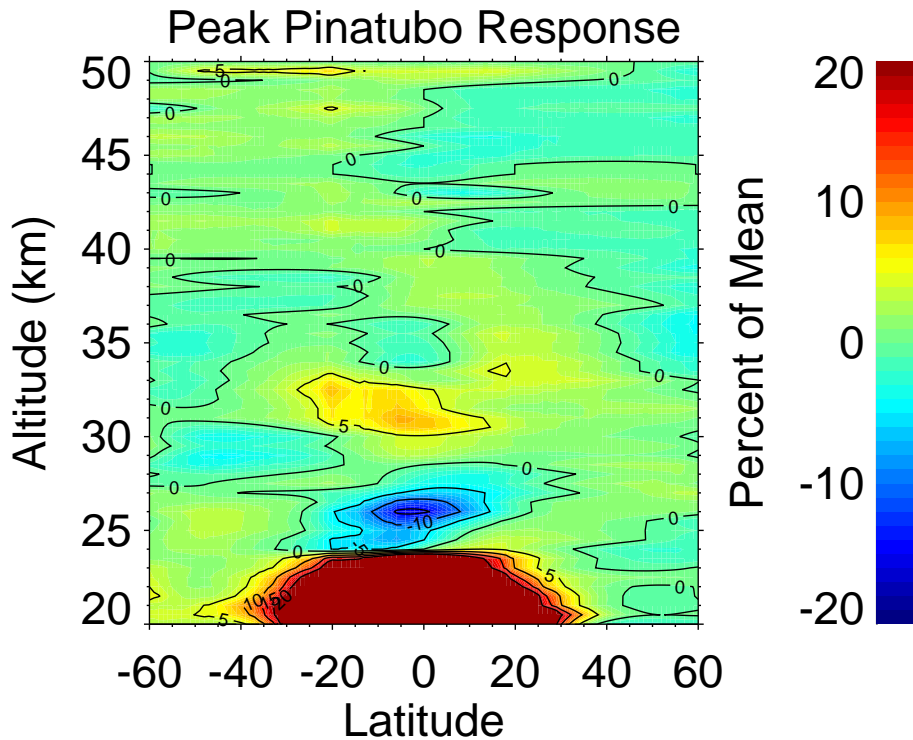


Figure 8. Peak of volcanic term near the time of Pinatubo as a percent of mean. Extraneously high values at lower altitudes are the result of overfitting to gaps in data as shown in Fig. 1.

Reevaluation of stratospheric ozone trends from SAGE II data

R. P. Damadeo et al.

Title Page

Abstract Introduction

Conclusions References

Tables Figures

◀ ▶

◀ ▶

Back Close

Full Screen / Esc

Printer-friendly Version

Interactive Discussion



Reevaluation of stratospheric ozone trends from SAGE II data

R. P. Damadeo et al.

Title Page

Abstract

Introduction

Conclusions

References

Tables

Figures



Back

Close

Full Screen / Esc

Printer-friendly Version

Interactive Discussion

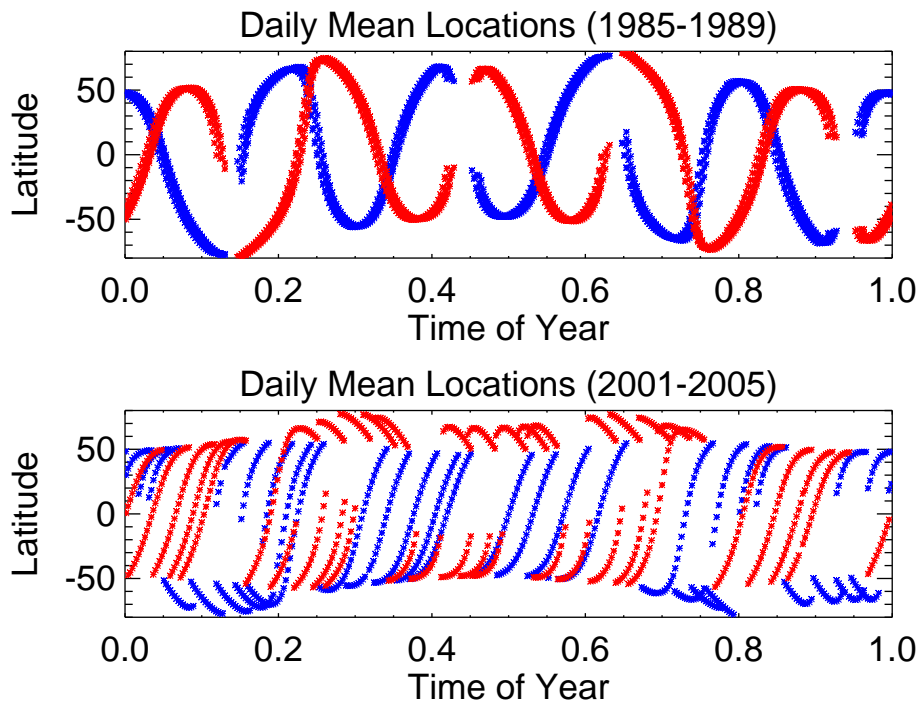


Figure 9. Locations of daily means for each satellite event type (sunrises are blue and sunsets are red) at the beginning and end of the mission.

Reevaluation of stratospheric ozone trends from SAGE II data

R. P. Damadeo et al.

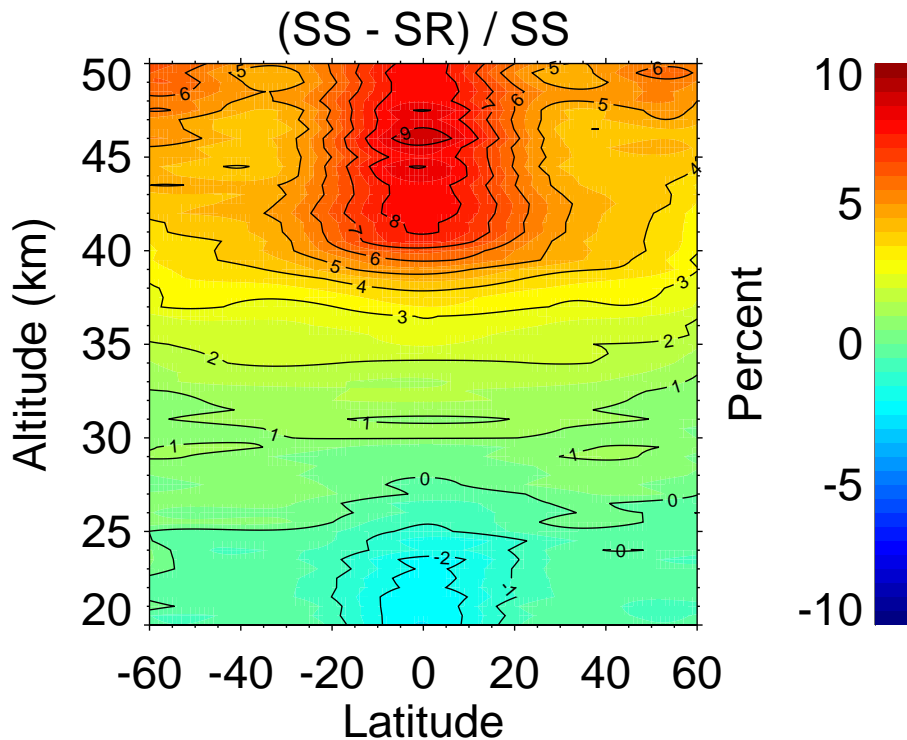
[Title Page](#)[Abstract](#)[Introduction](#)[Conclusions](#)[References](#)[Tables](#)[Figures](#)[◀](#)[▶](#)[◀](#)[▶](#)[Back](#)[Close](#)[Full Screen / Esc](#)[Printer-friendly Version](#)[Interactive Discussion](#)

Figure 10. Results of the local event type piece-wise term from the STS regression plotted as the percent difference between sunrise and sunset events.

Reevaluation of stratospheric ozone trends from SAGE II data

R. P. Damadeo et al.

Title Page

Abstract

Introduction

Conclusions

References

Tables

Figures



Back

Close

Full Screen / Esc

Printer-friendly Version

Interactive Discussion

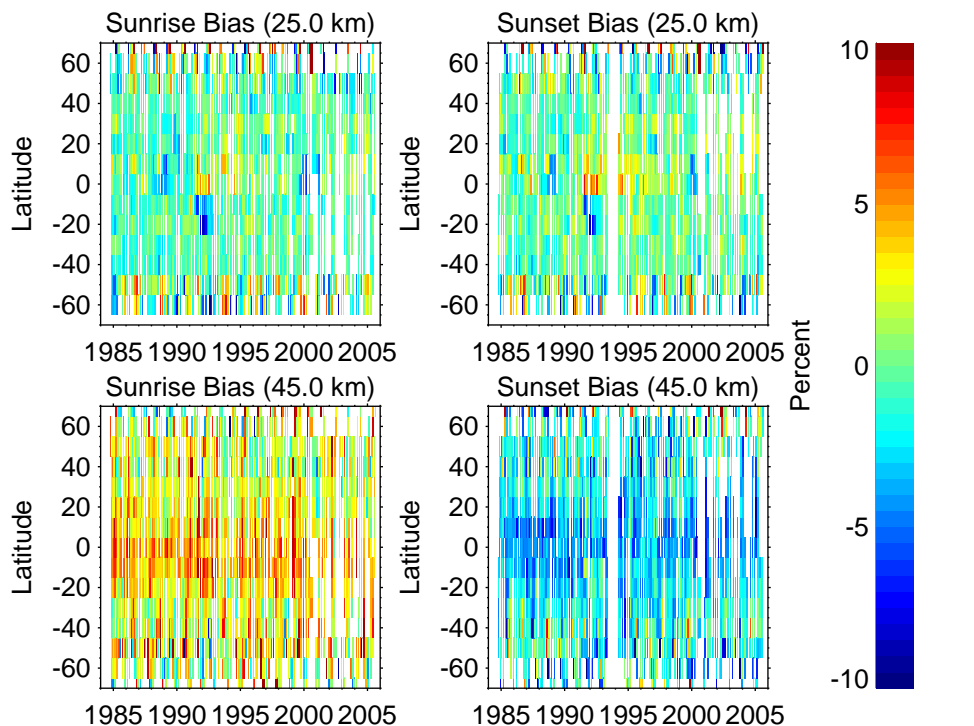


Figure 11. Biases for each monthly zonal mean for the MZM method compared to the STS method computed as $(MZM - STS)/STS \cdot 100$. The MZM method does not differentiate between event types so it does not have different values for each type. White areas show regions where data does not exist or where one or both regression methods failed to converge to a solution.

Reevaluation of stratospheric ozone trends from SAGE II data

R. P. Damadeo et al.

Title Page

Abstract

Introduction

Conclusions

References

Tables

Figures



Back

Close

Full Screen / Esc

Printer-friendly Version

Interactive Discussion

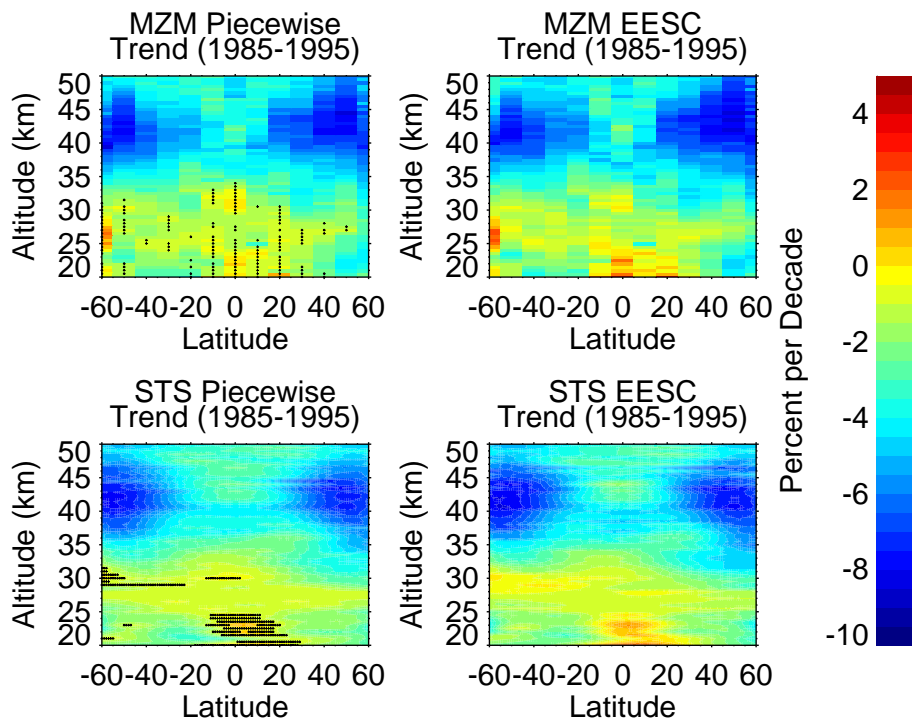


Figure 12. Mean trend between 1985 and 1995 for four analysis scenarios computed as $(Tr(1995) - Tr(1985))/Tr(1985) \cdot 100$ where $Tr(t)$ represents the value of the long-term trend term at time t . The analysis was run for both the MZM and STS regression methods, each using either a piece-wise linear term joined at 1997.0 or two orthogonal EESC terms. Stippling shows regions where the linear slope is not significant at the two-sigma level. No similar calculation can be done for multiple EESC terms.

Reevaluation of stratospheric ozone trends from SAGE II data

R. P. Damadeo et al.

Title Page

Abstract

Introduction

Conclusions

References

Tables

Figures

◀

▶

◀

▶

Back

Close

Full Screen / Esc

Printer-friendly Version

Interactive Discussion

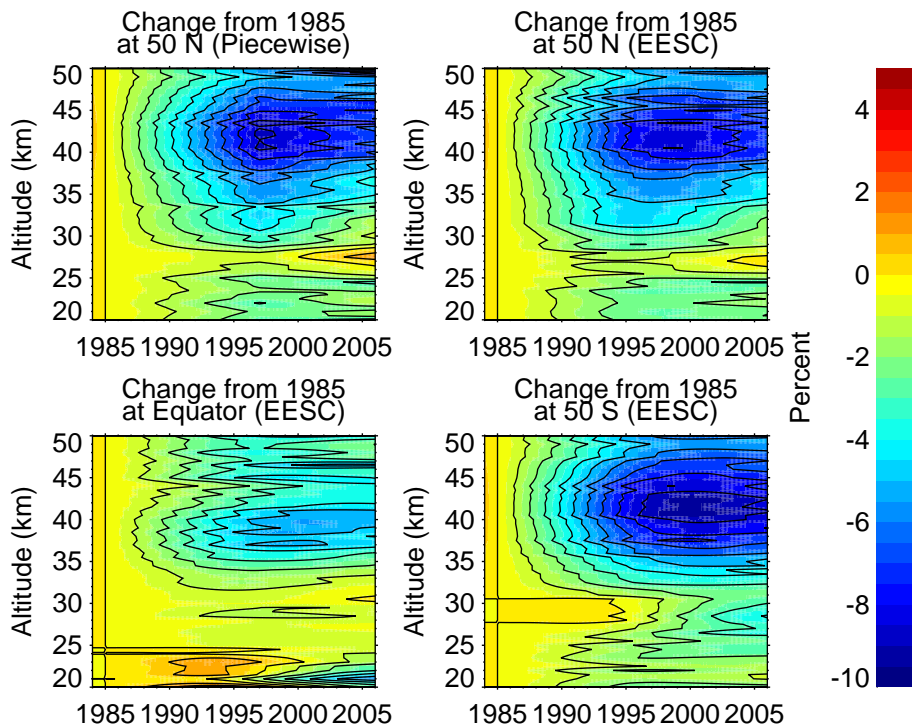


Figure 14. Some examples of the long-term trend term computed using the STS regression. The term in the top left comes from the use of a piecewise linear term while the other three come from the use of two orthogonal EESC terms. Contour intervals are 1%.

Reevaluation of stratospheric ozone trends from SAGE II data

R. P. Damadeo et al.

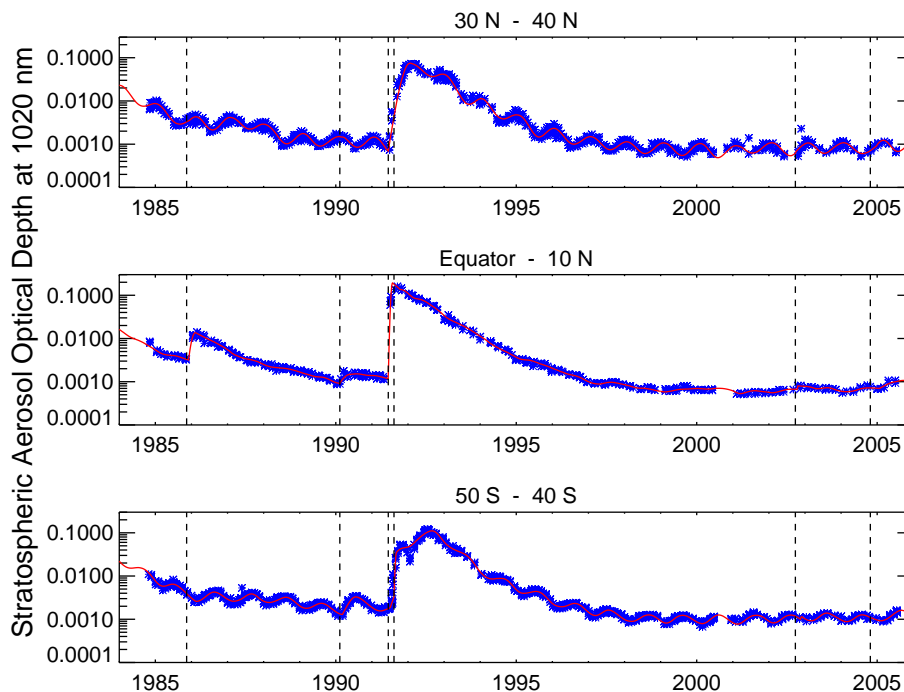
[Title Page](#)[Abstract](#)[Introduction](#)[Conclusions](#)[References](#)[Tables](#)[Figures](#)[◀](#)[▶](#)[◀](#)[▶](#)[Back](#)[Close](#)[Full Screen / Esc](#)[Printer-friendly Version](#)[Interactive Discussion](#)

Figure 15. Some examples of the non-linear fit to aerosol at three different center latitudes (35° N, 5° N, and 45° S). Data within each band are shown in blue while fits are shown in red. The vertical lines denote the times of the seven eruptions used for the fit (El Chichon is off scale). Note the difference in rates of rise and peak times at different latitudes, most easily visible for Pinatubo.

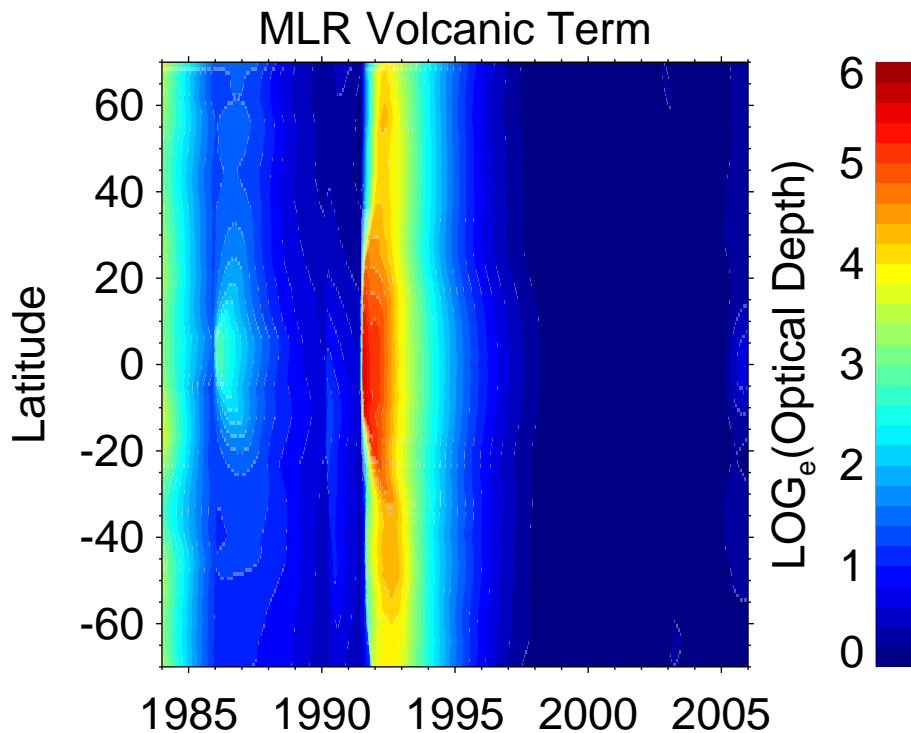


Figure 16. The volcanic term resulting from the STS regression to stratospheric aerosol optical depth in the 1020 nm channel. This is the term used as a volcanic proxy term for the regression to ozone data.

Reevaluation of stratospheric ozone trends from SAGE II data

R. P. Damadeo et al.

Title Page

Abstract Introduction

Conclusions References

Tables Figures

◀ ▶

◀ ▶

Back Close

Full Screen / Esc

Printer-friendly Version

Interactive Discussion

